Desalination and Water Treatment
www.deswater.com

doi:10.5004/dwt.2019.24485

165 (2019) 16–23
October

Simulation of a small solar storage tank and its operation strategy

Chen-Yi Tsai, Rome-Ming Wu*

Department of Chemical and Materials Engineering, Tamkang University, No. 151, Yingzhuan Rd., Danshui Dist., New Taipei City 25137, Taipei, Taiwan, email: molly21060@gmail.com (C.-Y. Tsai), Fax +886-2-26209887, email: romeman@mail.tku.edu.tw (R.-M. Wu)

Received 5 January 2019; Accepted 2 June 2019

ABSTRACT

An indirect solar thermal energy storage system has been developed to stabilize the solar energy supply. The thermal storage tank used in this paper has a volume of 61.6 L, with a cold-hot double coil placed within the tank. Hot fluid as a solar energy source at a temperature of 340 K was allowed to flow into the hot coil at a rate of 0.471 L/min, and cold fluid at a temperature of 300 K was allowed to flow into the cold coil at a rate of 0.094 L/min to satisfy daily use. Thermocouple meter readings were made to obtain temperatures at designated points within the storage tank and to get the temperature at the exit of the cold coil after it has gone through heating. The data obtained from the experiment were compared to those from the FLUENT simulation. By simulating various changes in the physical parameters of the hot and cold fluids, the intake temperatures of these fluids, the intake flow rate, and the contact area between the hot/cold coil pipes, the researchers analyzed the temperature classifications inside the storage tank as well as the outtake temperature of the cold fluid. In this small solar storage tank system, it can provide about 47°C, 113 L hot water during 5–9 pm in summer day, which is sufficient for daily use for a family with three persons. It is suggested that more better efficiency could be reached if hot fluid is replaced by high conductivity fluid owing to the benefit of the indirect contact system.

Keywords: Solar; Thermal stratification; Storage tank; Temperature; CFD

1. Introduction

Due to the increase of energy demanding and energy costs, thermal energy storage (TES) systems have become an alternative renewable energy sources [1–5]. Solar energy has the features of intermittency and low energy intensity. Although peak solar radiation occurs near noon, the peak energy demand is in the late evening, when solar radiation is unavailable. To address this problem, an indirect solar thermal energy storage system has been developed stabilize the solar energy supply. A storage tank is used to store the energy collected during daytime for nighttime use.

Furbo and Mikkelsen [6] found that thermal stratification can decrease the temperature at the collector intake, thus improving its efficiency. Moreover, it decreases the periods of operation of the auxiliary energy supply, which enhancing the efficiency of the water tank and the entire extended system. The improvement of stratification is limited when the aspect ratio of the length and the tank wall thickness exceeds 3.0, or the storage tank has an L/d value exceeding 200. Yoo and Pak [7] proposed a simple correlation of the efficiency as a function of the Peclet number in work. Previous studies also compared the fully stratified water tanks and fully mixed water tanks, and found that the energy storage efficiency of the system increased by 6–20% [8]. Jordan and Furbo [9] showed that increased thermal stratification can improve thermal performance of the system.

Previous studies used both experimental and numerical methods to examine the impact of stratification on 12 different baffle plates [10], and found that placing an obstacle in the tank provides better thermal stratification than when there is no obstacle. Heat exchangers that are placed inside or outside the storage tank can conduct indirect heat transfer [11]. The three indirect heat transfer methods include immersed coils exchanger, external shell-and-tube [12], and

*Corresponding author.

mantle-heat exchanger [13]. Increased flow rate and the area of heat exchange can improve heat transfer, but the lower initial temperature of the storage tank reduces the amount of thermal stratification. The efficiency of heat storage is also affected by the structure of the coil exchanger inside the tank. Spur et al. [14] proposed three structural designs for the immersed coil, and reached a difference of 15°C in temperature between the top and the bottom of the tank. Haller et al. [15] experimentally quantified the stratification of a storage tank.

Face of problems of traditional solar storage system, like large space needed, heat loss and unstable system performance, a solar heating system with a phase change material (PCM) thermal storage tank is investigated [16,17]. Recently, Sarbu and Sebarchievici [18] published a good review of sensible and latent heat storage systems like water tank, packed-bed, phase change materials, and heat pump systems.

This study used a cold/hot double coil, which differs from previous studies. As the hot and cold fluids were separated in the coil area, thermal stratification could be easily maintained. Moreover, the proposed design does not need to maintain the same flow of hot and cold fluids for avoiding agitation of fluid in the tank. In the example of membrane distillation desalination [19,20], which used sea water as a cold fluid, and heated the sea water by hot water inside the tank once it entered the tank. Oil-based fluids with fast heat transfer were used as the hot fluid for heating up the water inside the storage tank.

CFD simulation has been widely used to solve the three-dimensional models [21–24]. Hence, this study uses a validated CFD program (FLUENT) to design a thermal storage tank. The results of FLUENT were compared with the experimental system.

2. Experimental set-up

2.1. Structure of the thermal storage tank

Fig. 1 shows the structural diagram of the inside of a solar storage tank. The tank was measured with a height of 49 cm and a diameter of 40 cm. Both of its coils had the same dimension and size and were placed opposite each other on the left and right sides inside the tank. The overall coil diameter measured 10 cm. The coil pipe had a pipe diameter and thickness of 1 and 0.1 cm, respectively, and with total height of 35 cm. The coil on the right side of Fig. 1 is where hot fluid (water) from the thermal collector passes through, and the pipe coil on the left side is where the cold fluid passes through. Hot fluid entered into the hot coil to provide heat to the water inside the tank. The heat was then transferred to the cold coil. To make things simpler, the thermal collector was substituted with a thermostatic bath, so that hot fluid entering the tank can be kept at a certain intake temperature.

Cold fluid, with the help of a pump and flow meter, entered into the storage tank. After the temperature of the cold fluid was raised by the heat exchanger, the cold fluid was ready to be used. The hot fluid first had to reach 340 K inside the thermostatic bath before the experiment started, in which the hot fluid had to pass through the flow meter before it entered the coil inside the tank. Stainless steel coil

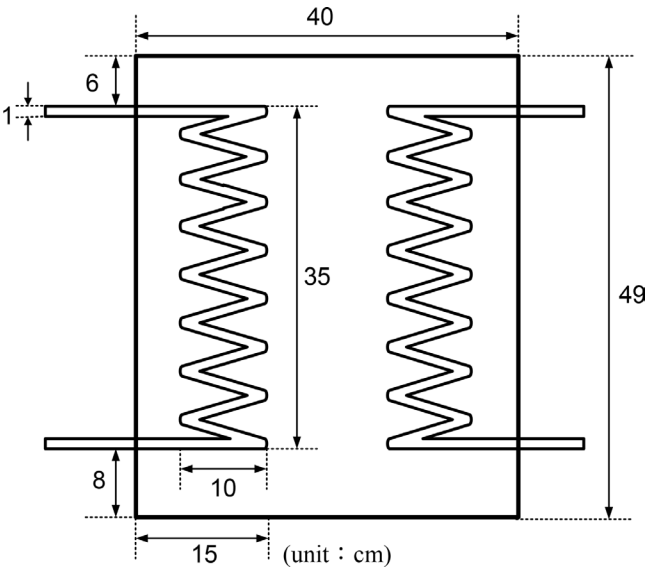

Fig. 1. Structural diagram of solar storage tank.

pipes were used to transfer the heat energy to the working fluid inside the tank, allowing the temperature of the fluid inside the tank to gradually rise and producing thermal stratification as a result. Hot fluid that had cooled due to heat dissipation after leaving the storage tank was made to flow back into the thermostatic bath for reheating.

2.2. Temperature measurement

The storage tank and its hot and cold coils were all made of stainless steel. The tank was clad in insulation material, shielding it from external heating. The insulation thickness was selected by the manufacturer. The iron plates covering the top of the tank 10 cm away from the center of the tank in the up, down, left, and right directions were designated N, S, C, and H, respectively. Four points were available where thermocouple meters could be positioned to measure the temperature at each point inside the tank. Thermocouple meters at each position could measure up to five temperature points, at distances of 8, 17, 26, 35, and 44 cm respectively from the bottom of the tank. A total of 20 temperature points could be measured this way. C1 represents the temperature point located at 44 cm from the bottom of the tank, where the thermocouple meter is positioned in the left direction; with C2 at 35 cm, C3 at 26 cm, C4 at 17 cm, and C5 at 8 cm from the bottom of the tank. N, S, and H are similarly listed, as shown in Fig. 2.

2.3. Experimental procedure

First, the storage tank was filled with hot water at a temperature of 310 K. Thermocouple meters were then placed at designated positions above, below, left, and right, relative to the center of the tank. The experiment then commenced. The pump was activated, cold fluid was poured into the cold flow pipe, and hot fluid was directed into the hot flow pipe through the thermostatic bath. The temperature at each point was recorded every 15 min for the three-hour duration of the experiment. Afterward, the initial tempera-

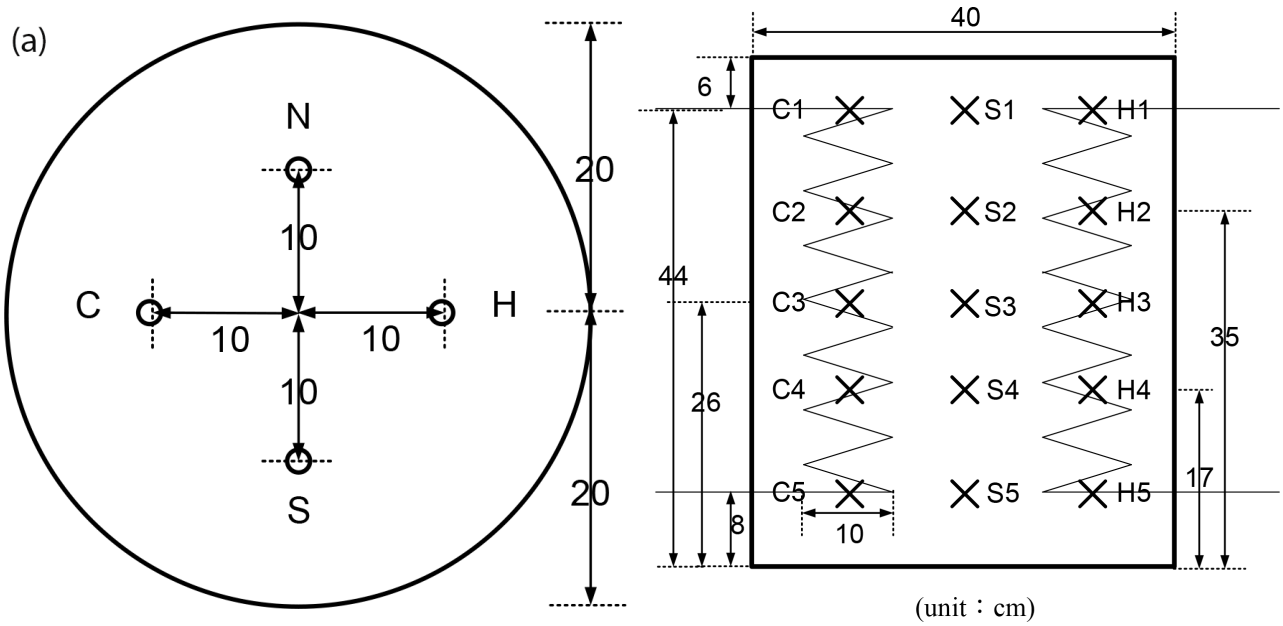

Fig. 2. (a) vertical view of the storage tank (b) side view of the storage tank.

ture inside the tank was adjusted to 320 K, and the aforementioned experimental steps were repeated.

3. Numerical methods

3.1. Geometry and meshes

The geometry and meshes of the thermal storage tank are displayed in Fig. 3. The T-grid mesh volumes used in this study were about 500,000 (Fig. 3). There were 9780 coil grids. Grid independence studies were then conducted, and it was determined that once the number of elements were halved and doubled, the numerical solutions of the average temperature showed a maximum difference of 3.9% between consecutive grids. CFD transient simulations were carried out using a small time-step of 10 s and a set of fine body-fitted computational grids. The results of FLUENT were then verified against the same experimental system, with the results exhibiting a high level of correlation.

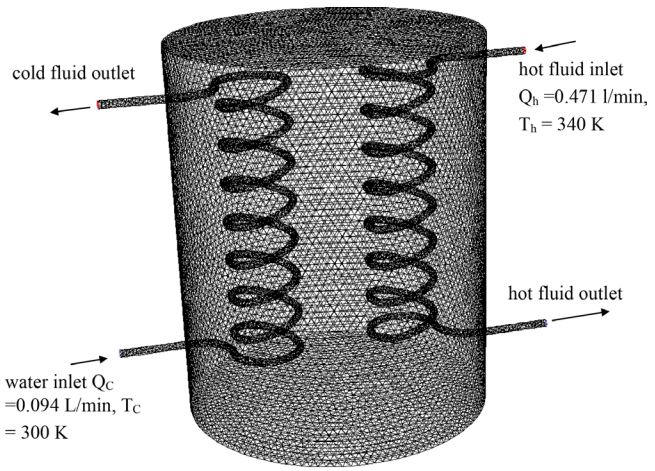

Fig. 3. Grid diagram used in the simulated solar storage tank.

3.2. Initial and boundary conditions

The PRESTO and second-order upwind methods were used for the discretization of the pressure and the momentum equations. The SIMPLE algorithm was employed to treat the pressure-velocity coupling. Cold water flowed at a rate of 0.02 m/s into the coil at the bottom of the tank at a temperature of 300 K. Hot water flowed at a rate of 0.1 m/s into the coil at the top of the tank at a temperature of 340 K. The fluids inside the tank were set to a constant temperature of 310 K. The small storage tank is considered as an insulated system. The governing equations, initial and boundary conditions are as follows:

$$\rho\frac{D\upsilon}{Dt} = -\nabla P + \mu\nabla^2\upsilon + \rho g \tag{1}$$

$$\rho Cp\frac{DT}{Dt} = K\nabla\ \upsilon \tag{2}$$

$$T_{tank} = \ constant \tag{3}$$

$$v_c = v_h = \ constant, v_{wall} = 0 \tag{4}$$

$$T_c = T_h = \ constant \tag{5}$$

where Eqs. (1) and (2) denote momentum and energy balance equation, respectively. Eq. (3) states that the initial temperature of the tank fluid is constant. Eq. (4) states that velocity of fluid in cold and hot coil are constant, while at any walls meets no slip boundary condition. Eq. (5) describes that temperature of fluid in cold and hot coil are constant.

The simulations started from zero velocity with the solution of the energy equation disabled, so as to get an initial velocity field. The simulations continued while considering heat transfer and buoyancy effects. The solution is considered convergent if the scaled residuals for the continuity equation, the momentum equation, and the energy equation are less than 1.0×10^{-4}, 1.0×10^{-4}, and 1.0×10^{-7}, respectively. One typical simulation takes approximately 12 h for a computer with a 3 GHz CPU processor and 1GB of memory.

4. Results and discussion

4.1. At a hot fluid intake temperature of 340 K and initial tank temperature of 310 K

Fig. 4 shows the XZ sectional view of the temperature stratification inside the tank 120 min after hot and cold sea water passed into the tank. The dark-blue color on the left side of the color plot represents the lowest temperature, at 300 K. The red color represents a temperature of 340 K. Fluid with a lower temperature will fall to the bottom of the tank, with the temperature moving higher towards the upper level of the tank. The temperature of the cold water coil pipe gradually increased from 300 K at the bottom intake to about 315 K, while the temperature of the hot fluid coil pipe fell from a temperature of 340 K at the intake position to 328 K at the outtake position.

Fig. 5 illustrates the change in temperature over time at different heights inside the tank. The X-coordinates represent temperature points at various dimensionless heights inside the whole tank. The Y-coordinates represent absolute temperatures. Starting from the bottom of the tank, temperature points were placed at increments of 3.5 cm, for a total of 13 temperature points. Simulations were carried out at 60, 120, and 180 min for comparisons with the experimental diagram. The temperature of the hot fluid was 340 K; the flow rate into the hot coil pipe was 0.471 L/min; the temperature of the cold fluid was 300 K; the flow rate into the cold coil pipe was 0.094 L/min; and the initial temperature of the fluid inside the storage tank was set to 310 K. The

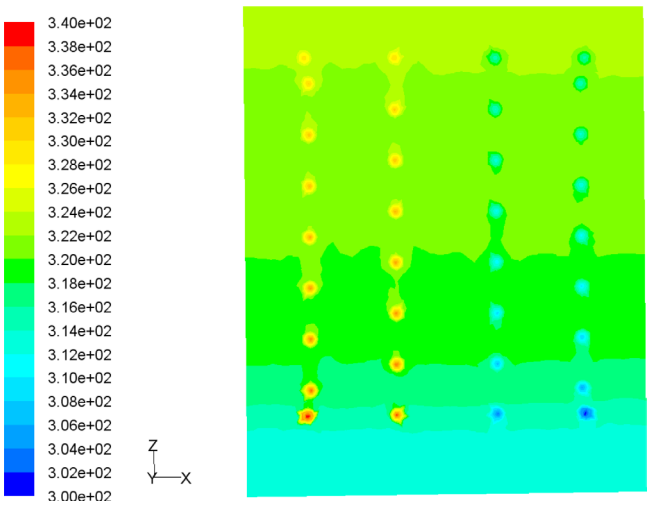

Fig. 4. Comparison of XZ section view of temperature stratification at 120 min.

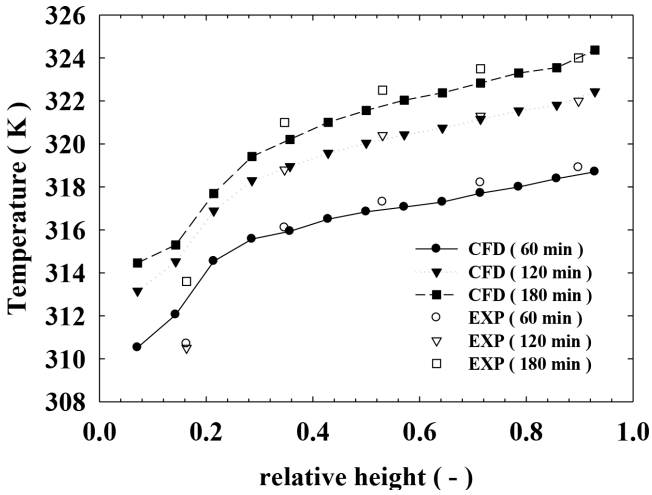

Fig. 5. Comparison of temperature measurements and simulations at various heights inside the storage tank (initial tank temperature of 310 K, temperature of hot fluid at 340 K, temperature of cold fluid at 300 K

solid dots were temperature data points recorded at various heights using Fluent simulation. The open dots were data obtained during the experiment. It can be seen that the data from the experiment were consistent with the simulation.

Fig. 6 shows the positions of the points 17 cm from the bottom of the tank - C4, H4, S4, and N4 - as measured by the experiment, and the change over time of the temperature points at the 35 cm positions (C2, H2, S2, and N2). It can be seen in the storage tank that when the heights are the same, the temperatures are also the same. Therefore, subsequent discussions will only focus on the changes in the temperature at positions of different height.

4.2. Various initial tank temperatures with the intake temperature of hot fluid set to 340 K

Fig. 7 presents that if the initial temperature of the storage tank is set to 300, 310, or 320 K and the inlet temperatures of cold and hot fluids remain the same as before

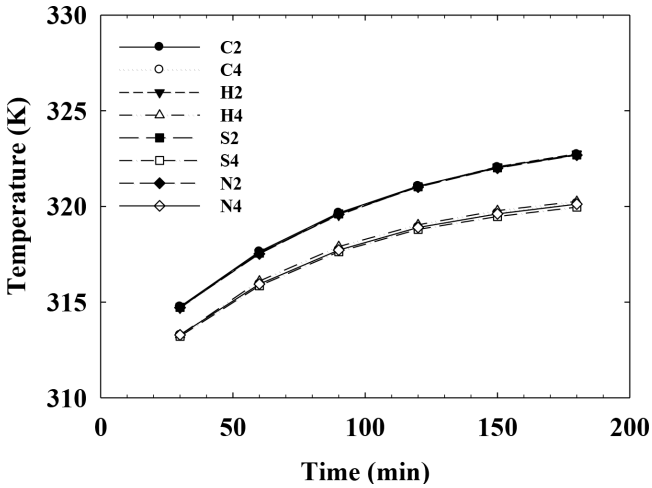

Fig. 6. Temperature of storage tank at heights of 17 and 35 cm.

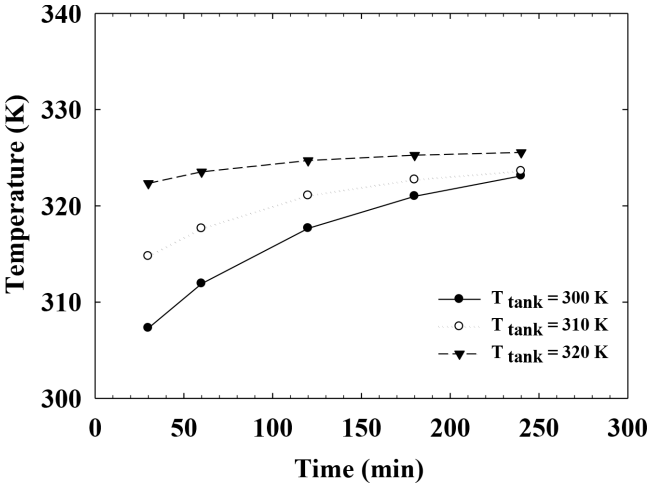

Fig. 7. Comparison between initial tank temperature change and the temperature at C2.

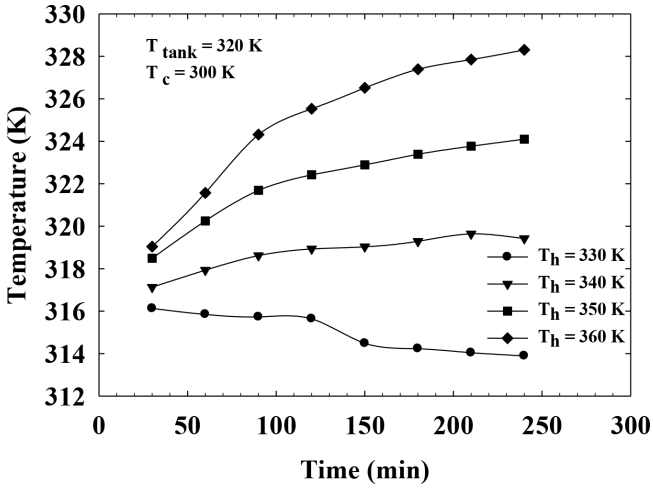

Fig. 8. Comparison between hot fluid temperature change and the temperature at C2, when the initial tank temperature is 320 K.

(hot fluid at 340 K and cold fluid at 300 K), then a higher initial storage tank temperature hastens the stabilization of the tank temperature. The cold outtake temperature also increases, especially when the tank temperature is maintained at 320 K. This can provide a stable cold fluid temperature at the outtake.

4.3. Changing the hot fluid intake temperature with an initial tank temperature of 320 K

Fig. 8 demonstrates the change in temperature at C2 over time for intake temperatures of 330 K, 340 K, 350 K, and 360 K, with an initial tank temperature of 320 K. When the temperature of the hot fluid was fixed at 330 K, the temperature at C2 dropped to about 314 K due to a lack of sufficient heat. When the temperature of the hot fluid was fixed at 340 K, 350 K, and 360 K, the temperature at C2 gradually stabilized to 319 K, 324 K, and 328 K, respectively, after 180 to 240 min. When the initial tank temperatures were constant and the hot fluid intake temperature was higher, the temperature at C2 also increased.

4.4. Changing the intake flow rate of cold fluid

Fig. 9a shows a fixed intake flow rate of hot fluid of 0.471 L/min, a temperature of 340 K, and an initial tank temperature set to 310 K. The three different cold fluid flow rates were 0.094 L/min, 0.236 L/min, and 0.471 L/ min; the in take temperature was 300 K. With the change in the outtake temperature of the cold fluid over time, after 4 h, as the flow rate of cold fluid increased, the outtake temperature became 317 K, 312 K, and 307 K for each corresponding flow rate. Obviously, as the flow rate at the cold fluid intake increases, the heat energy inside the tank is siphoned away more quickly, leading to lower temperatures inside the tank; sometimes up to 10 degrees lower. In contrast, even though there was no change in the cold fluid parameters, Fig. 9b shows that with an increase in the hot fluid flow rate, the cold outtake temperatures became 313 K, 316 K, and 318 K, respectively. Although a faster flow rate at the hot fluid intake can provide more heat energy to the tank and thereby raise the tank temperature, the cold outtake temperature increased by only about 5 K. As compared to the change in the flow rate of the cold fluid, the changes to the temperature due to changes

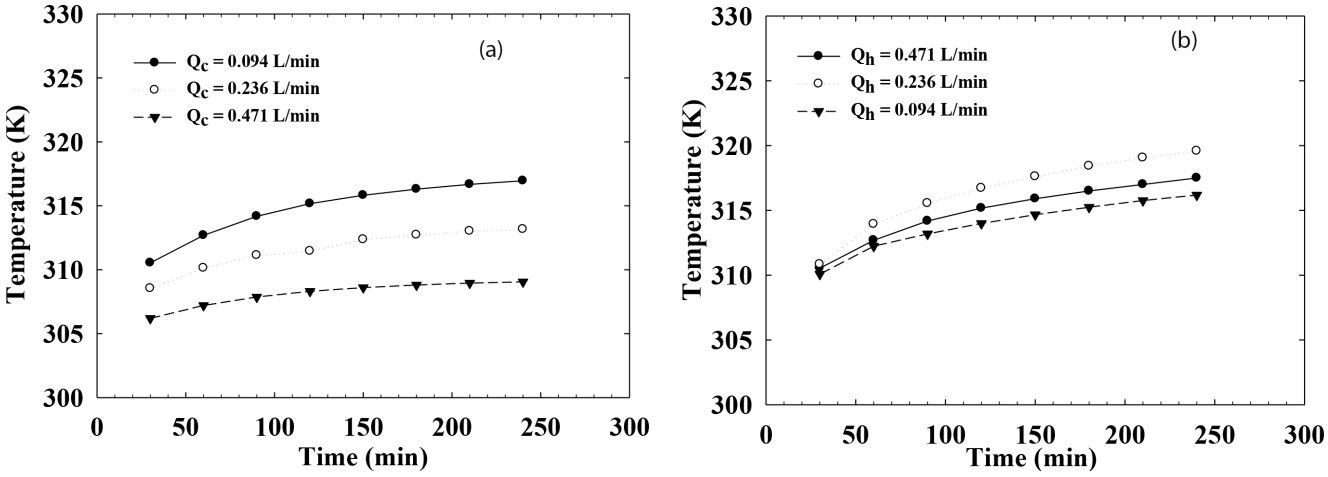

Fig. 9. Outlet temperature at 120 min of changing flow rates of (a) cold and (b) hot coil fluids.

in the flow rate of the hot fluid were significantly smaller. Therefore, a larger load demand (meaning the addition of more heat to the cold fluid) necessitated maintaining or improving the temperature of the storage tank, rather than increasing the flow rate of the hot fluid.

4.5. Changing the radii of the hot and cold coil pipes

In order to understand the heat transfer efficiency of the thermal storage system, the radii of the hot and cold coil pipes were changed to increase the area of heat transfer. In Fig. 10, the solid dots represent the temperature distribution of the hot and cold coil pipes with a radius of 0.5 cm. When the radius of the cold coil pipe was increased to 0.75 cm (open circle), the temperature at points inside the tank dropped by about 2.5 K. Comparably, when the radius of the hot coil pipe was increased to 0.75 cm while maintaining the same radius of the cold coil pipe (solid triangle), it raised the tank temperature by about 5 K. However, when the radii of both the hot and cold coil pipes were increased to 0.75 cm (open triangle), the resulting curve overlaps with the one in which the radii of the hot and cold coil pipes were 0.5 cm. Simultaneously changing both radii did not result in any change to the tank temperature. Thus, to make the heat transfer of the thermal storage system more efficient, the radius of the hot coil pipe could be increased.

4.6. Changing the number of loops in the hot and cold coil pipes

Another way to increase the heat transfer area is to raise the number of loops in the cold and hot coil pipes. Fig. 11 shows that when the number of loops in the hot coil pipes remains the same while the number of loops in the cold coil is changed from 8 to 12, the temperature of the entire tank drops as a result of the increased heat energy being siphoned away by the cold coil. Compared to the set-up with the original cold coil pipe of 8 loops, the temperature of the tank dropped by about 1 more degree (the open circular dots). In addition, when the number of loops in the hot coil pipe is also increased to 12, a comparison of the simultaneous increase in the number of loops of both the cold and hot coil pipes to the original cold and hot coil pipes of only 8 loops indicated that the resulting three curves almost overlap. It means that there was no significant increase in tank temperature; thus, increasing the number of loops in the hot coil pipe cannot effectively increase the tank temperature.

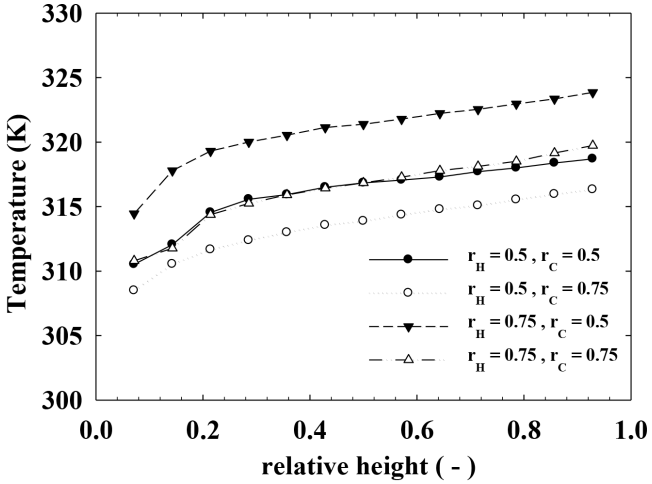

Fig. 10. Change in tank temperature when the radii of cold and hot coils are different.

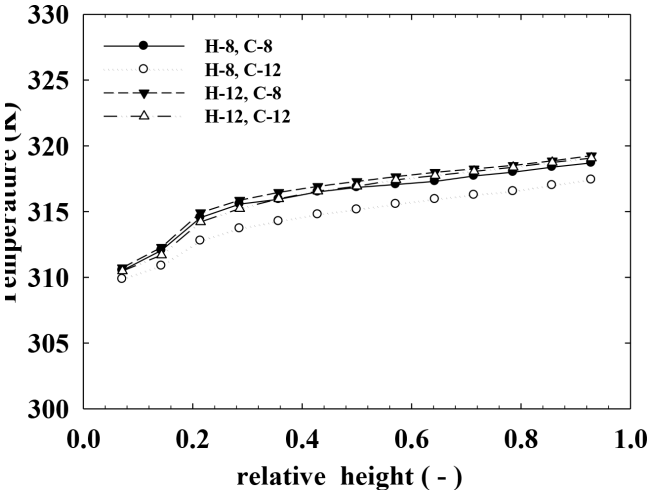

Fig. 11. Change in various tank temperatures under the changing number of loops in cold and hot coils.

4.7. Hot and cold fluids entering separately

To simulate the performance of the storage tank from afternoon to evening, two water-inducing methods were simulated. The first part simulated the in-flow of hot fluid, where the in-flow rate of this fluid was 0.471 L/min at a temperature of 340 K. The flow of cold fluid was initially suspended. The next part of the simulation suspended the flow of hot fluid, and the flow setting of the cold fluid was then initiated. The intake flow rate of cold fluid was 0.094 L/min at an intake temperature of 300 K. Both parts were simulated for 4 h, and the results were compared to the situation in which hot and cold fluids flow simultaneously.

Fig. 12 illustrates the comparison of various in-tank temperatures between the situation in which there is only an inflow of hot fluid while the flow of cold fluid is suspended, and the situation in which both the cold and hot fluids flow simultaneously. After 180 min, the temperature in the tank resulting from the inflow of only hot fluid is 4 K higher on average than when both fluids flow simultaneously. The inflow of only hot fluid was simulated for 4 h, after which the flow of hot fluid was suspended, and then cold fluid began to flow. Based on these results, if the demand for water in a summer afternoon is not high, then the temperature inside the tank can be increased by 4 K.

4.8. Changing the intake temperature of the hot fluid at 30-min intervals

To better describe the temperature of the hot fluid collected by the thermal collector during a summer afternoon,

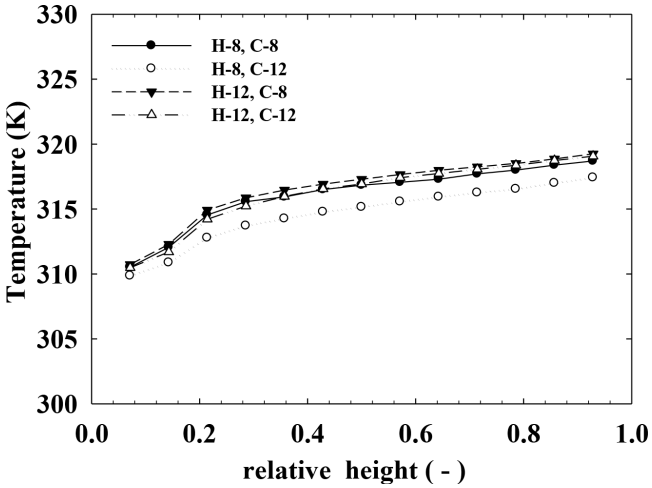

Fig. 12. Temperature distribution in the tank under different heating strategy.

the intake temperature of the hot fluid was changed every 30 min. From an initial temperature of 330 K, the hot fluid reached its highest temperature of 360 K at 210 min and finally dropped to 340 K, with a total simulation time frame of 8 h. The temperature change of the supplied hot fluid is shown in Fig. 13 (solid triangle).

As can be seen in Fig. 13, the maximum outtake temperature of cold fluid can reach 328 K (open circle), which is far higher than the outtake temperature of 317 K achieved when the intake temperature of the hot fluid was fixed at 340 K (solid circle). If the 8-h simulation were to start from 9 am, then by approximately 12:30 pm the temperature of the hot fluid from the collector could have reached its highest temperature of 362 K. By continuing the simulation for another 1.5 h, when the clock strikes 2:00 pm, the temperature of the cold fluid could reach as high as 328 K. This indicates that the results of previous simulations regarding constant heat flow temperature underestimated the cold flow temperature. That cold water can actually be heated from 310 K to 328 K (nearly 55°C) might be inspiring news.

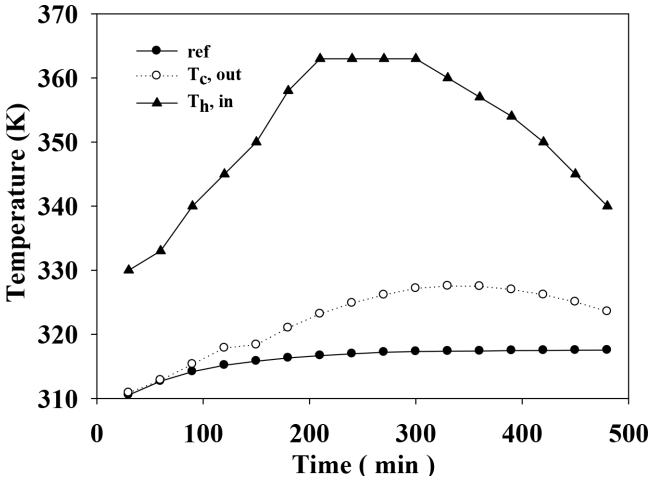

Fig. 13. Temperature distribution in the tank during a summer afternoon.

5. Conclusions

This research aims to provide a small thermal storage system with indirect contact heat transfer type. This is a preliminary attempt, at present, the experiment has verified the feasibility of numerical simulation, and provides summer day operation mode. Followings are some conclusion points till now. Generally speaking, the time of heat exchange is lengthened, thermal stratification becomes greater. IF the initial temperature of the storage tank increases while the intake temperature of the hot fluid remains the same, the temperature stabilizes sooner. The tank temperature and the cold fluid outtake temperature also increase. In addition, the load for the cold fluid becomes larger, the more appropriate action is to maintain or improve the storage tank temperature or increase the radius of the hot fluid coil, rather than increase the flow rate of hot fluid. It is suggested that if the thermal fluid used in the simulated system is altered from water to fluid with a higher heat transfer coefficient, then the cold flow temperature should improve further.

Acknowledgements

The authors would like to thank the National Science Council of the Republic of China, Taiwan, for financially supporting this research under Contract No. NSC 98-2621-M-032-003.

References

[1] Y. Taamneh, A. Al-Shyyab, Improvement of the performance of a solar still by utilizing the sorption thermal storage of natural zeolite, Desal. Water Treat., 57(57) (2016) 27450–27457.
[2] M. Moser, F. Trieb, T. Fichter, J. Kern, Renewable desalination: a methodology for cost comparison, Desal. Water Treat., 51(4–6) (2013) 1171–1189.
[3] A.E. Kabeel, E.M.S. El-Said, Development strategies and solar thermal energy utilization for water desalination systems in remote regions: a review, Desal. Water Treat., 52(22–24) (2014) 4053–4070.
[4] G.L. An, L.W. Wang, J. Gao, Two-stage cascading desorption cycle for sorption thermal energy storage, Energy, 174 (2019) 1091–1099.
[5] Y. Konuklu, F. Erzin, H.B. Akar, A.M. Turan, Cellulose-based myristic acid composites for thermal energy storage applications, Sol. Energ. Mat. Sol. C., 193 (2019) 85–91.
[6] S. Furbo, S.E. Mikkelsen, Is low-flow operation an advantage for solar heating systems? Proc. ISES Solar World Congress, 1 (1987) 962–966.
[7] H. Yoo, E.T. Pak, Theoretical model of the charging process for stratified thermal storage tanks, Solar Energy, 51 (1993) 513–519.
[8] N.K. Ghaddar, Stratified storage tank influence on performance of solar water heating system tested in Beirut, Renew Energy, 4 (1994) 911–925.
[9] U. Jordan, S. Furbo, Thermal stratification in small solar domestic storage tanks caused by draw-offs, Solar Energy, 78 (2005) 291–300.
[10] N. Altuntop, M. Arslan, V. Ozceyhan, M. Kanoglu, Effect of obstacles on thermal stratification in hot water storage tanks, Appl. Therm. Eng., 25 (2005) 2285–2298.
[11] Y.M. Han, R.Z. Wang, Y.J. Dai, Thermal stratification within the water tank, Renew. Sust. Energ. Reviews, 13 (2009) 1014–1026.
[12] K.F. Fraser, K.G.T. Hollands, A.P. Brunger, An empirical model for natural convection heat exchangers in SDHW systems, Solar Energy, 55 (1995) 75–84.

[13] G.L. Morrison, A. Nasr, M. Behnia, G. Rosengarten, Analysis of horizontal mantle heat exchangers in solar water heating systems, Solar Energy, 64 (1998) 19–31.
[14] R. Spur, D. Fiala, D. Nevrala, D. Probert, Performance of modern domestic hot-water stores, Appl. Energ., 83 (2006) 893–910.
[15] M.Y. Haller, E. Yazdanshenas, E. Andersen, C. Bales, W. Streicher, S. Furbo, A method to determine stratification efficiency of thermal energy storage processes independently from storage heat losses, Solar Energy, 84 (2010) 997–1007.
[16] M. Kenisarin, K. Mahkamov, Solar energy storage using phase change materials, Renew. Sust. Energ. Reviews, 11 (2007) 1913–1965.
[17] J. Zhao, Y. Ji, Y. Yuan, Z. Zhang, J. Lu, Energy-saving analysis of solar heating system with PCM storage tank, Energies, 11 (2018) 237–254.
[18] I. Sarbu, C. Sebarchievici, A comprehensive review of thermal energy stirage, Sustainability, 10 (2018) 191–222.
[19] S. Adnan, M. Hoang, H. Wang, Z. Xie, Commercial PTFE membranes for membrane distillation application: Effect of micro structure and support material, Desalination, 284 (2012) 297–308.
[20] S.S. Ray, S.S. Chen, D. Sangeetha, H.M. Chang, C.N.D. Thanh, Q.H. Le, H.M. Ku, Developments in forward osmosis and membrane distillation for desalination of waters, Environ. Chem. Lett., 16(4) (2018) 1247–1265.
[21] M. Nataraj, R.R. Singh, Analyzing pump impeller for performance evaluation using RSM and CFD, Desal. Water Treat., 52(34–36) (2014) 6822–6831.
[22] M. Nataraj, R.R. Singh, Analyzing pump impeller for performance evaluation using RSM and CFD, Desal. Water Treat., 52(34–36) (2014) 6822–6831.
[23] A. Tamburini, G.L. Barbera, A. Cipollina, G. Micale, M. Ciofalo, CFD prediction of scalar transport in thin channels for reverse electro dialysis, Desal. Water Treat, 55(12) (2015) 3424–3445.
[24] R. Sengur, G. Deveci, R. Kaya, T. Turken, S. Guclu, D.Y. Imer, I. Koyuncu, CFD modeling of submerged membrane bioreactors (sMBRs): a review, Desal. Water Treat., 55(7) (2015) 1747–761.